Tu4.4 INTENSITY-DEPENDENT BEAT FREQUENCY IN A FIBEROPTIC RING LASER GYRO

S. Huang, L. Thévenaz*, K. Toyama, B. Y. Kim**, and H. J. Shaw

Edward L. Ginzton Laboratory, Stanford University, Stanford
California 94305, USA

* Swiss Federal Institute of Technology, Laboratoire de Métrologie
1015 Lausanne, Switzerland

** Advanced Institute of Science & Technology, Yusung-ku
Taejon, Korea

I. Introduction

The Kerr effect causes a nonreciprocity between the two counterpropagating lightwaves in the fiber coil of a fiberoptic gyro, thus resulting in a spurious rotation signal.[1-4] For interferometric fiber gyros, a power difference as small as ten nanowatts gives a rotation error which is too large for inertial navigation. In this paper, we describe properties of the Kerr effect as observed in a Brillouin fiber-optic gyro (BFOG).

II. Description of the BFOG System

Figure 1 shows the schematic diagram of the experimental Brillouin fiber-optic ring laser gyro. It consists of three 1.3 μm-wavelength fused-type directional couplers constructed of non-PM single-mode optical fiber. These couplers are spliced together at points S. Coupler C_1 splits the input light into two parts, P1 and P2, with nominally equal power, while C_2 and C_3 have weak power coupling (~a few percent). A laser-diode-pumped 1.32 μm Nd:YAG ring laser is the pump source.

By means of polarization controllers PC1 and PC2, the polarizations of the pump waves P1 and P2 within the cavity are adjusted to coincide with an eigen-polarization of the cavity. Two Brillouin waves B1 and B2 are produced by P1 and P2 inside the cavity as long as the circulating power levels of P1 and P2 are above the Brillouin threshold. Here only first order Brillouin waves are assumed to be excited. The Brillouin beat note appears at the output of detector D_1. Because of reciprocity, little pump power is received at D_1 as long as P1 and P2 excite the same eigen-polarization mode in the cavity with well-balanced power.

The coil diameter is ~ 20 cm. The total fiber cavity length is ~27 m including the parts wound on the two PZTs. The finesse is 75, free spectral range is ~ 7.6 MHz, and cold cavity (i. e. below Brillouin threshold) linewidth is ~ 100 kHz. We limit the pump level to values below the second-Stokes threshold so that only first-Stokes waves are excited. The first-Stokes pump threshold at the entrance to the cavity is ~ 0.376 mW. The frequency of the first-Stokes waves is measured to be down-shifted from the pump frequency by 12.8 GHz.

III. Intensity-Dependent Beat Frequency in BFOG

In the ring laser cavity, the effective index for either Brillouin wave B1 or B2 is perturbed by the presence of both Brillouin waves and both pump waves through the Kerr effect. When all waves in the cavity are in the same eigenpolarization mode, the index perturbations δn for the two Brillouin waves are found from the basic field equations to be

Reprinted with permission from the 9th Optical Fiber Sensors Conference, Associazione Elettrotecnica ed Elettronica Italiana (Florence, 1993). © 1993 AEI.

$$\begin{cases} \delta n_{B1} = \alpha n_2 (P_{B1} + 2P_{B2} + 2P_{P1} + 2P_{P2}) / A_{eff} \\ \delta n_{B2} = \alpha n_2 (2P_{B1} + P_{B2} + 2P_{P1} + 2P_{P2}) / A_{eff} \end{cases} \quad (1)$$

where A_{eff} is the effective fiber-core area, n_2 is the nonlinear-index coefficient. For linear and circular polarizations, α = 1 and α = 2/3 respectively, and for elliptical polarizations, α ranges between these limits.[5] The P's denote power levels of circulating waves inside the cavity with subscripts denoting the various waves. Equations (1) can be interpreted as follows. The terms in P_{B1} and P_{B2} are the well-known self modulation terms (coefficient unity) and cross modulation terms (coefficient 2) for two oppositely propagating waves (in the absence of P_{P1} and P_{P2}) as found, for example, in the interferometric fiber gyro[4] and the passive resonator gyro[2] which have no waves corresponding to the pump waves here. The terms in P_{P1} and P_{P2} behave as cross modulation terms for both Brillouin waves, and therefore they all have coefficients of 2. From Eq. (1), a power imbalance $\Delta P_B = P_{B2} - P_{B1}$ between the Brillouin waves causes a differential index perturbation $\Delta n_B = \delta n_{B2} - \delta n_{B1}$ between waves B1 and B2. If f_{B1} and f_{B2} are respectively the clockwise (CW) and counter-clockwise (CCW) cavity resonant frequencies, a beat frequency bias $\Delta f_B = f_{B2} - f_{B1}$ occurs due to Kerr effect, where

$$\Delta f_B = -f_B \frac{\Delta n_B}{n_B} = \eta \Delta P_B \quad (2)$$

and

$$\eta = \frac{c\alpha n_2}{\lambda_B n_B A_{eff}} \quad (3)$$

where f_B and λ_B are respectively the average optical frequency and vacuum wavelength of the Stokes waves, and n_B is the refractive index.

IV. Kerr-Effect-Induced Beat Frequency Bias and Nonlinear Scale Factor

It can be seen that, in a BFOG system, a beat frequency bias will be induced by any input-pump-power imbalance because unbalanced P1 and P2 lead to unbalanced B1 and B2. As a result, the beat frequency response to the rotation rate for a BFOG will be shifted. The amount and sign of the beat frequency shift respectively depend on the amount and sign of the input-pump-power imbalance.

For the BFOG shown in Fig. 1, the beat frequency response to the rotation rate is not only shifted but also distorted because of the asymmetrical feedback arrangement for the cavity stabilization. Since this resonator cavity is stabilized by monitoring only P1 through coupler C_3 so that only the CCW resonance in the cavity coincides with the pump frequency. As rotation rate increases, the resonance frequency of the unstabilized CW cavity mode moves away from the pump frequency, decreasing the circulating cavity power of P2. This adds a component of pump power unbalance inside the cavity and a shift in beat frequency due to the Kerr effect, which increases as rotation rate increases. Thus this 'pump walk-off' leads to a nonlinear scale factor.

Fig. 2(a) describes the behavior of beat frequency vs. rotation rate in the presence of Kerr effect due to both initial pump-input imbalance plus pump walk-off. The straight line corresponds to an 'ideal' case in which there is no Kerr effect. With Kerr effect, the line is shifted down ($P_{P1,in} > P_{P2,in}$) or up ($P_{P1,in} < P_{P2,in}$), and also becomes curved. Since CCW and CW gyro rotations introduce beat frequencies of $\Delta f_B < 0$ and $\Delta f_B > 0$ respectively, the Kerr-effect-induced biases due to $P_{P1,in} > P_{P2,in}$ and $P_{P1,in} < P_{P2,in}$ are equivalent to CCW and CW rotations respectively, in terms of Eq. (2). The ends of the plots bend towards the CCW rotation direction, showing that P_{B2} becomes smaller with increased rotation rate. The beat signal disappears when the rotation rate reaches the value for which the circulating power of P2 becomes lower than the Brillouin threshold. Some experimental measurements with different input-pump-power imbalances have been done at our BFOG system. The unbalanced input-pump-power levels were

introduced by setting bending loss at points A1 and A2 (Fig. 1). $P_{P1,in}$ and $P_{P2,in}$ were measured using a non-invasive clamp-on microbending coupler (courtesy of Raynet Corp.). Figure 2(b) shows the difference between the measured beat frequency and the 'ideal' beat frequency as a function of rotation rate, which coincides with the expectation shown in Fig. 2(a).

V. Kerr-Effect Coefficient η

The Kerr-effect coefficient η determines the dependence of the Kerr-effect-induced bias on the power imbalance between the two Stokes waves inside the cavity according to Eq. (2). From Eq. (3) the theoretical values of η for our BFOG system are 76.1 Hz/mW for a linear eigen-polarization, 50.7 Hz/mW for a circular eigen-polarization, and 50.7 Hz/mW < η < 76.1 Hz/mW for an elliptical eigen-polarization where we have used $n_2 = 3.2 \times 10^{-16}$ cm²/W,[6] and $A_{eff} = \pi \times 4.565^2$ μm² (taking the fiber core radius as 4.15 μm and the V-number for wavelength of 1.32 μm as 2.29).

Experimental measurement of η requires a determination of Δf_B and ΔP_B. However, the latter is difficult to measure directly inside the cavity, without degrading the cavity finesse. Instead, we measure $P_{P1,in}$ and $P_{P2,in}$, and calculate the absolute circulating Stokes powers P_{B1} and P_{B2} through the formula[7]

$$P_B = P_P^{(th)}\left(\sqrt{\frac{P_{P,in}}{P_{P,in}^{(th)}}} - 1\right) \tag{4}$$

where '*(th)*' denotes pump threshold for first Stokes. We have ignored the position-dependence of P_B along the ring cavity, which is reasonable as long as the loss in one round-trip (including the coupling loss) is low. $P_{P,in}^{(th)}$ and $P_P^{(th)}$ in our BFOG system are 0.376 mW and 21 mW respectively.

From the experimental dependence of Δf_B on ΔP_B, invoking Eq. (4), we obtain the slope of the fitting line of Δf_B on ΔP_B, i. e. the average Kerr-effect coefficient η to be ~68.5 Hz/mW. This is in good agreement with the theoretical expectation, as the state of eigen-polarization in the resonant cavity is generally elliptical. This large Kerr coefficient implies a requirement on the power balance between the two internal Stokes waves to an accuracy in the range of a fraction of a mW for a low grade gyro to a few nW's for a high grade gyro.

This research was supported by Litton Systems, Inc.

References

1. S. Ezekiel, J. L. Davis, and R. Hellwarth, "Intensity dependent nonreciprocal phase shift in fiber gyro," in *proceedings of the first International Conference on Fiber-Optic Rotation Sensors and Related Technologies* (Springer-Verlag, New York), 1982, pp. 332-336
2. Katsumi Iwatsuki, Kazuo Hotate, and Minoru Higashiguchi, "Kerr effect in an optical passive ring-resonator gyro," *J. Lightwave Technol*, vol. LT-4, pp.645-651 (1986)
3. Koichi Takiguchi and Kazuo Hotate, "Partially digital-feedback scheme and evaluation of optical Kerr-effect induced bias in optical passive ring-resonator gyro," *IEEE Photon. Technol. Lett*, vol. 3, pp. 679-681 (1991)
4. R. A. Bergh, H. C. Lefevre, and H. J. Shaw, "Compensation of the optical Kerr effect in fiber-optic gyroscopes," *Opt. Lett*, vol. 7, pp. 282-284 (1982)
5. R. A. Bergh, *Ph. D Dissertation*, Stanford University, Chapter 4 (1983)
6. Govind P. Agrawal, *Nonlinear Fiber Optics*, Academic press Inc, San Diego, Calif. 1989, pp. 183
7. P. Bayvel and I. P. Giles, "Evaluation of performance parameters of single-mode all-fiber Brillouin ring lasers," *Opt. Lett*, vol. 14, pp. 581-583 (1989)

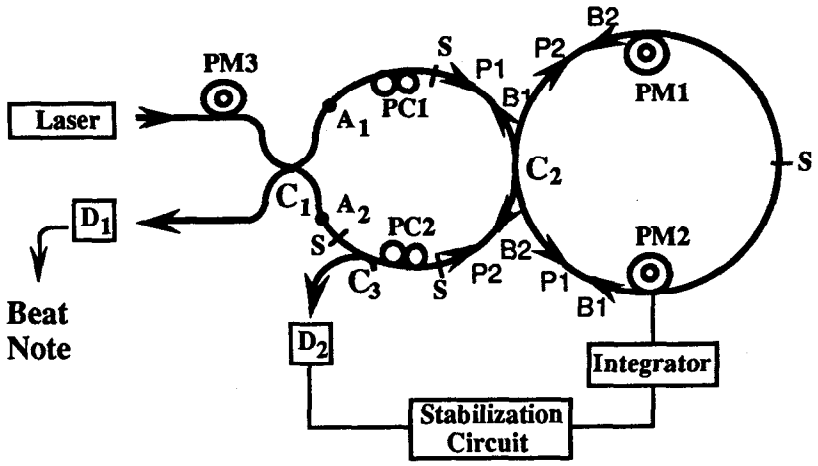

Figure 1. Schematic diagram of the BFOG system: P1 and P2, pump waves; B1 and B2 Brillouin waves.

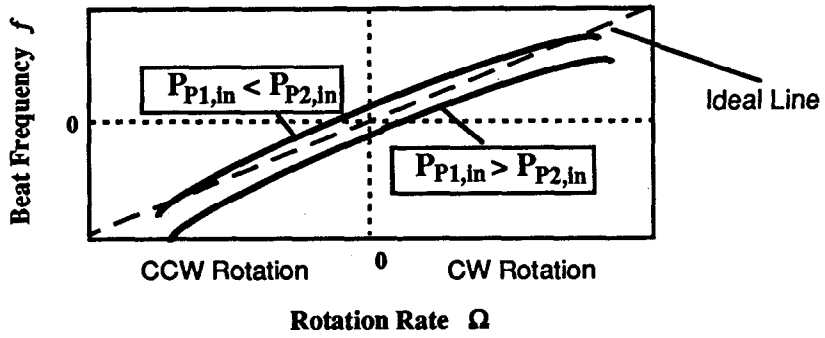

(a)

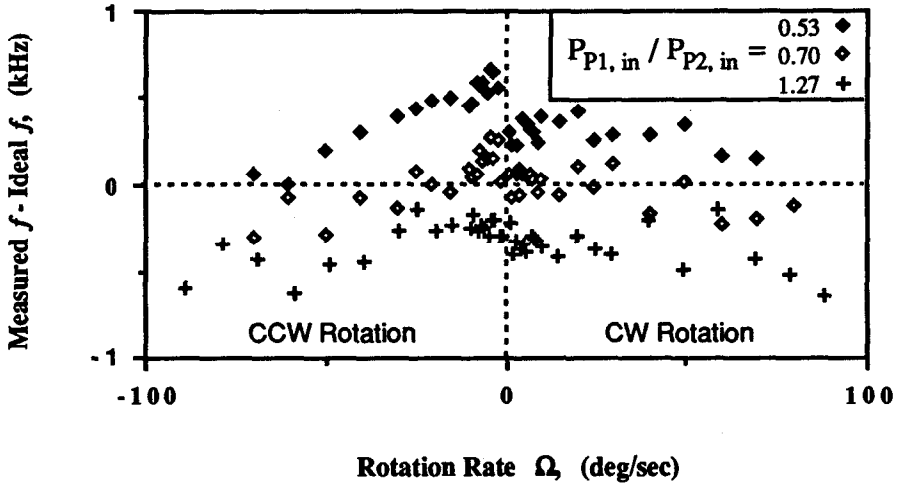

(b)

Figure 2. (a) Dependence of beat frequency on rotation rate under Kerr effect;
(b) Difference between measured beat frequency and 'ideal' beat frequency vs. rotation rate.